ADVANCED MATERIALS TECHNOLOGIES
www.advmattechnol.de

Chitosan-Based, Biocompatible, Solution Processable Films for In Vivo Localization of Neural Interface Devices

Onni J. Rauhala, Soledad Dominguez, George D. Spyropoulos, Jose Javier Ferrero, Talia R. Boyers, Patricia Jastrzebska-Perfect, Claudia Cea, Dion Khodagholy, and Jennifer N. Gelinas**

Chitosan (CS) is a biocompatible, inexpensive organic polymer that is increasingly used in neural tissue applications. However, its intrinsic fluorescence has not yet been leveraged to facilitate localization of neural interface devices, a key procedure to ensure accurate analysis of neurophysiological signals. A process is developed to enable control of mechanical and chemical properties of CS-based composites, generating freestanding films that are stable in aqueous environments and exhibit concentration-dependent fluorescence intensity. The shape and location of CS-coated probes are reliably visualized in vitro and in vivo using fluorescence microscopy. Furthermore, CS neural probe marking is fully compatible with classical immunohistochemical and histological techniques, enabling localization of high spatiotemporal resolution surface electrocorticography arrays in adult rats and mouse pups. CS composites have the potential to simplify and streamline experimental procedures required to efficiently acquire, localize, and interpret neurophysiological data.

Organic materials are increasingly being used to interface with live tissue because of their enhanced biocompatibility and preferable chemical and mechanical properties compared to conventionally used inorganics.[1–4] Chitosan (CS) is one such material that has gained traction for use in multiple biomedical applications due to its unique biological profile. It is a naturally occurring, abundant polysaccharide that is biocompatible, bio-adhesive, and antimicrobial.[5–8] Furthermore, living cells can be safely exposed to CS and its enzymatic degradation products without adverse effects.[8,9] It is solution processable and film forming, allowing for incorporation of additives and tuning of properties. CS also exhibits intrinsic fluorescence, although it is typically coupled with conjugate fluorescent targets to permit use as a sensing probe.[10,11]

CS is increasingly being used in applications involving neural tissue, functioning as a component of hydrogels for neural tissue engineering and nanoparticles for neurologic drug delivery.[12–15] Recently, it has also been incorporated into neural interface devices.[7,16,17] Generally, neural interface devices are critical for transducing neural signals and form the basis for neurophysiological experimentation. Such devices are placed on the surface of the brain, or implanted to reach deeper structures.[18–20] Although neural interface devices can be placed stereotactically and neural activity patterns can provide clues as to the anatomical localization of electrodes in some cases, histological verification of electrode placement in specific brain structures is an important confirmation of experimental technique. Because cortical circuits and subcortical nuclei can be functionally differentiated on the scale of hundreds of micrometers,[21,22] knowing the precise location of electrodes is critical for proper interpretation of recorded neural activity.

Current methods for visualization of neural interface device placement include use of fluorescent dyes, immunologic tissue staining, and electrolytic lesions.[23–27] Fluorescent dyes such as (1,1′-dioctadecyl-3,3,3′,3′-tetramethylindocarbocyanine perchlorate (DiI), 3,3′-dioctadecyloxacarbocyanine perchlorate (DiO′) can be used to coat devices that are subsequently penetrated into neural tissue.[28,29] These lipophilic dyes become fluorescent when incorporated into the neural membrane and undergo noncovalent binding. Although reliable device localization can be attained with this method, these dyes have the potential to affect cell function.[30] Immunologic tissue staining (Nissl, glial fibrillary acidic protein) relies on visualizing the tissue damage that results from a penetrating device, leading to high variability of response and poor spatial resolution.[31–33]

O. J. Rauhala, Dr. S. Dominguez, Dr. J. J. Ferrero, T. R. Boyers, Prof. J. N. Gelinas
Institute for Genomic Medicine
Columbia University Irving Medical Center
New York, NY 10032, USA
E-mail: jng2146@cumc.columbia.edu
O. J. Rauhala, Dr. G. D. Spyropoulos, P. Jastrzebska-Perfect, C. Cea, Prof. D. Khodagholy
Department of Electrical Engineering
Columbia University
New York, NY 10027, USA
E-mail: dk2955@columbia.edu
Prof. J. N. Gelinas
Department of Neurology
Columbia University Irving Medical Center
New York, NY 10032, USA
The ORCID identification number(s) for the author(s) of this article can be found under https://doi.org/10.1002/admt.201900663.

DOI: 10.1002/admt.201900663

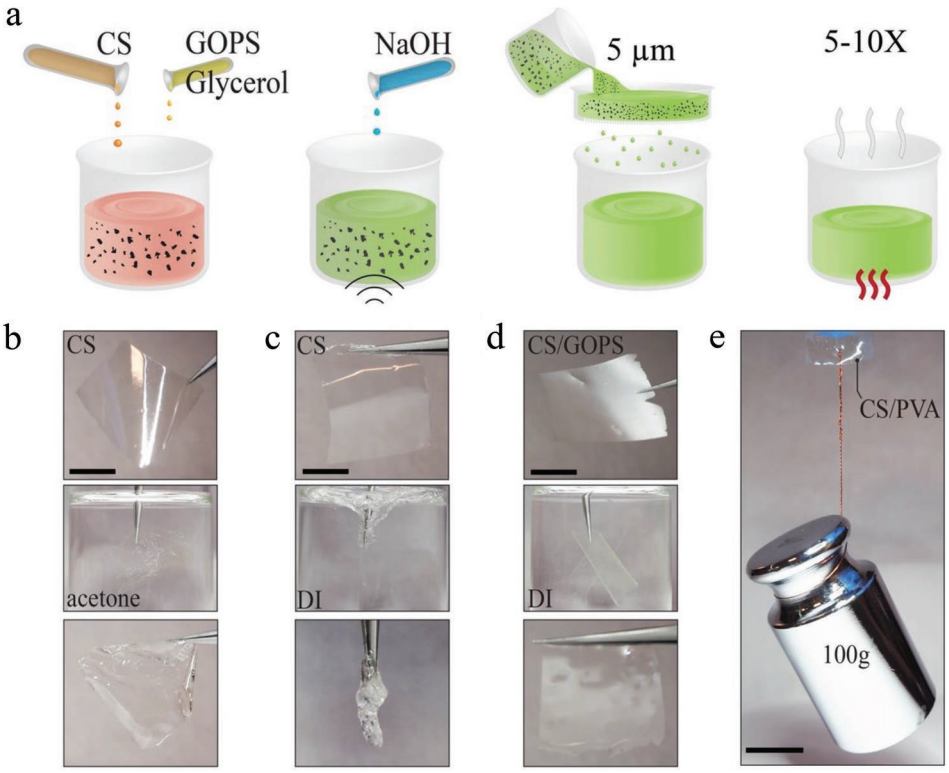

Figure 1. Creation of freestanding, stable, mechanically robust CS-based films. a) Schematic of CS solution processing. b) Mechanical stability of freestanding CS film before and after acetone immersion. Scale bar 1 cm. c) Mechanical stability of freestanding CS film before and after DI water immersion. Scale bar 1 cm. d) Mechanical stability of freestanding CS/GOPS film before and after DI water immersion. Scale bar 1 cm. e) Mechanical resilience of freestanding CS/PVA film experiencing a downward force of 0.98 N. Scale bar 2 cm.

In addition, such tissue responses are increasingly being minimized by use of flexible, smaller neural interface devices. Electrolytic lesioning uses application of current to the brain at the site of the device, and relies on immunologic tissue staining to visualize the tissue response.[34] This approach is limited in that it induces brain damage and the extent of damage is difficult to control, also limiting spatial resolution.

We hypothesized that a biocompatible, low-cost, CS-based solution possessing sufficient intrinsic fluorescence for visualization could be generated and introduced into neural tissue. To test this hypothesis, we first developed a process that enables control of mechanical and chemical properties of CS-based composites. This process generated films that were stable in the presence of organic solvents often used in microfabrication processes, and had a controllable dissolution rate in aqueous environments. We characterized fluorescence intensity of films at varying concentrations of CS to identify the optimal concentration for visualization. In vitro implantation of CS-coated probes established the ability to reliably visualize probe penetration at different depths. Lastly, we validated the use of CS as a biocompatible in vivo neural interface device marker in the cortex of adult rat and developing mouse. CS-based composites can be integrated with classical immunohistochemical and histological techniques, as well as multiwavelength fluorescence imaging.

To investigate the applicability of CS and its composites to use with neural interface devices, we characterized the processability, stability, and mechanical reliability of the CS-based films. Our first goal was to create a freestanding CS-based film with a controllable dissolution rate in aqueous environments. We prepared a chitin solution by dissolving CS powder in 2% acetic acid solution, added a plasticizer (glycerol), and neutralized the pH by titrating 100×10^{-3} M NaOH solution with 100 μL steps. The solution was then sonicated for 1 h. The majority of CS products have high amounts of impurities and particles that preclude formation of a homogenous thin film. To remove these impurities, we prepared a six to ten times diluted solution and filtered it using a vacuum assist system. The lower viscosity of the diluted solution made this process possible. We then concentrated the solution on a stirring hot plate at 180 °C to reach the desired CS concentration (**Figure 1**a). Additionally, heating has been demonstrated to increase strength of CS fluorescence, potentially through altering the size of micelles formed.[11] This purified and amplified solution can be mixed with a variety of additives for tuning the desired chemical and mechanical features. CS solution can be cast on nonadhesive surfaces and heated to form freestanding films. Such films are able to maintain mechanical integrity and are chemically resistant to organic solvents typically used in microfabrication processes, such as acetone (Figure 1b). Addition of different concentrations of the cross-linking agent (3-glycidyloxypropyl) trimethoxysilane (GOPS) enabled precise control of CS dissolution rate in aqueous environments. When 2% GOPS was added to the CS solution, resultant films were nondissolvable in aqueous solution (Figure 1d). In the absence of GOPS or at low GOPS concentrations, film dissolution was observed

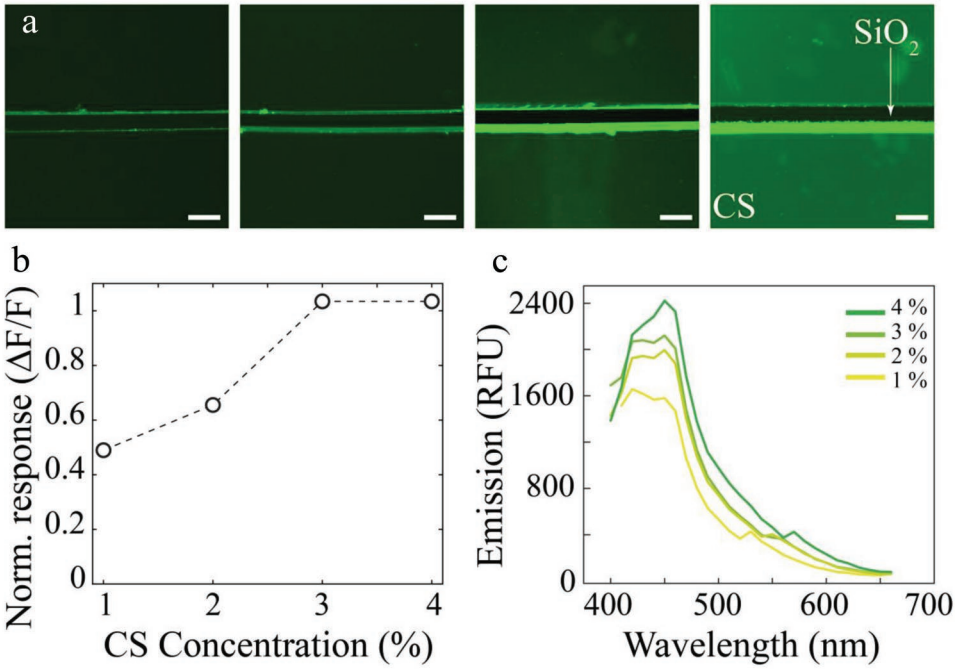

Figure 2. Characterization of CS intrinsic fluorescence. a) Fluorescence microscopy images of 1%, 2%, 3%, and 4% w/v CS films (left to right) scratched in the middle to reveal the underlying SiO_2 slide for consistent contrast. Scale bar 200 µm. b) Fluorescence intensity of CS increases with increasing solution concentration. c) Fluorescence spectra of CS solutions with different concentrations.

(Figure 1c). We also investigated CS film dissolution, with and without varying concentrations of GOPS, in deionized (DI) water, acetone, and phosphate buffered saline (PBS). GOPS stabilized the CS films over days in both an organic solvent and physiologic conditions (Figure S1, Supporting Information). The ability to control stability in aqueous environments is a powerful feature that can potentially be exploited to control in vivo drug delivery and tissue marking. To modulate mechanical stability, we added polyvinyl alcohol (PVA) to CS solution at a 1:1 ratio. This composite was physically robust and able to withstand significant mechanical forces (Figure 1e).

We then examined the fluorescent properties of the CS solutions. Fluorescence increased linearly with solution concentration, but no further increase in fluorescence intensity occurred when the concentration surpassed 3% w/v (**Figure 2**a,b). These results are consistent with the relationship reported for solutions of CS polymer.[11] Of note, CS oligomers express a decrease in fluorescence intensity when greater than 0.5% w/v solutions are used.[10] Fluorescence emission spectra revealed a broad peak with maximum at 450 nm (Figure 2c). Therefore, intrinsic CS fluorescence is optimally visualized with a green filter.

Localization of neural interface devices in brain tissue requires spatial resolution on the order of 50–200 µm to distinguish individual electrode or probe tracts. We introduced CS solution into agar gel with similar mechanical properties to brain (3% w/v) using penetrating probes with different cross-sectional areas to investigate the spatial resolution of its fluorescence. These penetrating probes were coated with CS solution, inserted a fixed depth (5 mm) into agar, and then removed (**Figure 3**a). Fluorescence microscopy of cross-sectional slices of this agar revealed that CS fluorescence tracked the diameter and shape of the probe used (Figure 3b,c). Fluorescence generated by blunt tipped 50 µm wire was punctate, whereas it was ring-shaped when a 313 µm needle was used. In both cases, the shape and fluorescence intensity was maintained at superficial and deep cross-sectional layers of the agar (Figure 3b,c bottom). As predicted by fluorescence emission spectra, CS introduced into agar was best visualized with a green filter, and fluorescence was reduced by 60% when blue or red filters were used. These results suggest that CS-based neural probe localization could be combined with immunohistochemical assays employing other wavelengths.

Next, we tested CS fluorescence in in vivo brain tissue. A CS-coated needle was inserted into the brain perpendicularly to the dorsal cortical surface of a rat, and then immediately removed, using stereotaxic micromanipulators. In order to extract brain tissue for processing, animals are typically perfused with paraformaldehyde (PFA), which can disrupt the binding and localization of fluorescent markers.[30] The tissue is then sliced into sections using a microtome or vibratome (**Figure 4**a). We found that CS was unaffected by the perfusion of PFA and slicing processes, clearly marking only the tissue surrounding the needle insertion point in a 100 µm thick brain slice. In addition, we investigated the compatibility of CS with other fluorescent markers by staining CS-marked brain tissue with 4′,6-diamidino-2-phenylindole (DAPI; Figure 4b). This fluorescent stain is extensively used in fluorescence microscopy due to its ability to pass through cell membranes and strongly bind to DNA.[35] Overlay of blue and green filtered images of rat brain tissue revealed intact DAPI staining of neurons and easily visible CS fluorescence marking the needle insertion point (Figure 4c). Therefore, CS is compatible with the techniques and chemicals routinely used during histological experimentation.

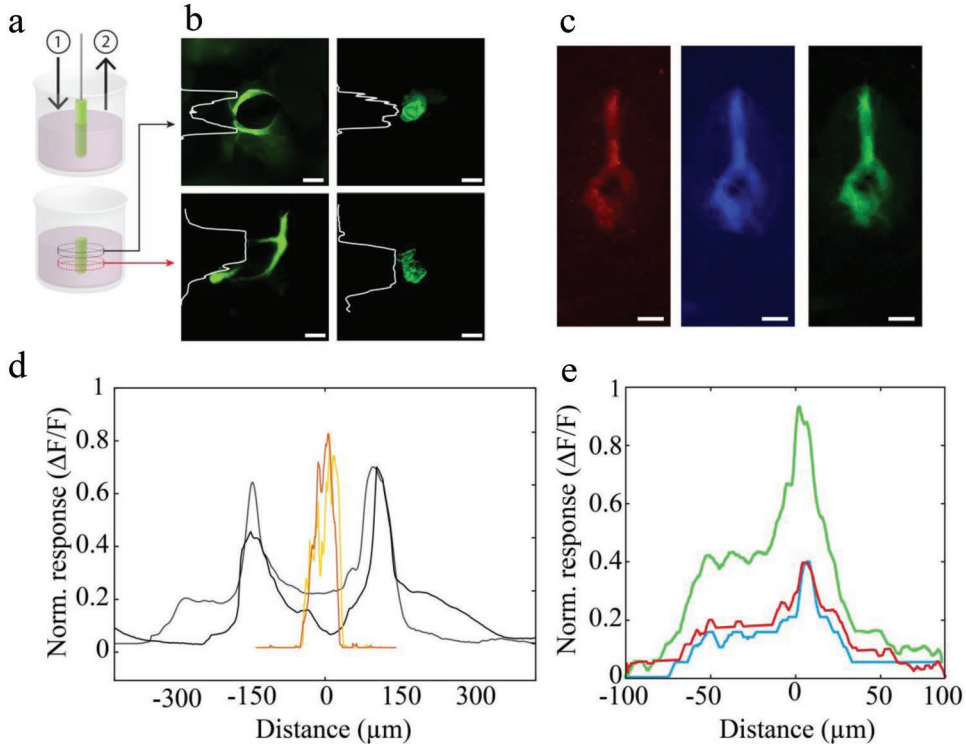

Figure 3. CS fluorescence marks the shape and location of probe implantation in vitro. a) Schematic for CS-coated probe insertion into agar (left). b) Fluorescence microscopy images of superficial (top row) and deep (bottom row) agar slices after insertion of CS-coated 30 gauge needle (left column) and 50 μm wire (right column). Scale bar 300 μm left, 50 μm right. c) Multiwavelength fluorescence microscopy images of CS-coated probe implantation into obliquely sectioned agar slice. Scale bar 300 μm. d) Fluorescence intensity across cross-sectional agar slice implanted with CS-coated 30 gauge needle (black = superficial slice, blue = gray slice) and CS-coated 50 μm wire (orange = superficial slice, yellow = deep slice), with distance = 0 μm corresponding to the midpoint of probe implantation. e) Multiwavelength fluorescence intensity across (left to right) obliquely sectioned agar slice in (c) with distance = 0 μm corresponding to the linear track of fluorescence.

Given this stability to tissue processing, we aimed to use CS for localization of neural interface devices used during acute in vivo electrophysiology. One of the most effective approaches to recording neural signals from multiple brain regions simultaneously is to employ surface electrocorticography arrays. Such arrays carry the added benefit of not penetrating into the brain and damaging fragile tissue.[23,26,27,36] However, these features also create challenges for localizing the position of the array, potentially limiting interpretation of neural signals acquired. We use a conformable conducting polymer-based electrocorticography array, the NeuroGrid, to record high spatiotemporal resolution electrophysiological data from the surface of the brain in adult rats and developing mice (postnatal days 5–14; Figure 4d). We investigated the applicability of CS for localizing these arrays on the surface of the rodent brain. At the conclusion of neurophysiological experimentation, a stereotactic arm was used to insert CS-coated needles into the rodent brain at the anterior or lateral corners of the NeuroGrid array. After perfusion of the rodent with PFA, brain tissue was extracted. To localize a surface array, tissue slices must be taken parallel to the cortical surface (axial slices). This process is complicated by the curvature of the cortex, necessitating removal of the deep midline brain structures and flattening of the cortex prior to slicing (Figure 4a).[37] Flattened 50 μm thick slices that preserved the relationships between regions on the cortical surface were generated. In order to reconstruct the position of the NeuroGrid, a tissue marker must be introduced into tissue depth, as the surface of cortex is often difficult to preserve during the slicing procedure. To obtain landmarks for specific cortical regions, we performed vGLUT2 immunohistochemistry on the tissue slices. vGLUT2 is a vesicular glutamate transporter that is strongly expressed by glutamatergic projection neurons from the thalamus, leading to a characteristic increase in expression in rodent primary somatosensory and visual cortices.[38,39] Expression of this transporter results in a particularly identifiable pattern in rodent barrel cortex, the brain region that processes sensory information from the whiskers, because these neurons are arranged in a densely packed ring that represents each whisker surrounding a hollow area that contains few neurons.[40] Imaging of vGLUT2 expression using fluorescent antibodies permits identification of rodent primary somatosensory and visual cortices (Figure 4e). We combined vGLUT2, DAPI, and CS fluorescence imaging in the flattened rodent brain slices and were able to visualize the location of the NeuroGrid array relative to cortical regions (Figure 4f). In this manner, we allocated recording electrodes to individual cortical regions, permitting multi-regional spatial analysis (Figure 4g).

To address the compatibility of the CS with neural tissue, we examined neuron-scale resolution images of the regions where CS was introduced into the brain. We did not find evidence of neuron loss or gliosis compared with control regions (Figure S2,

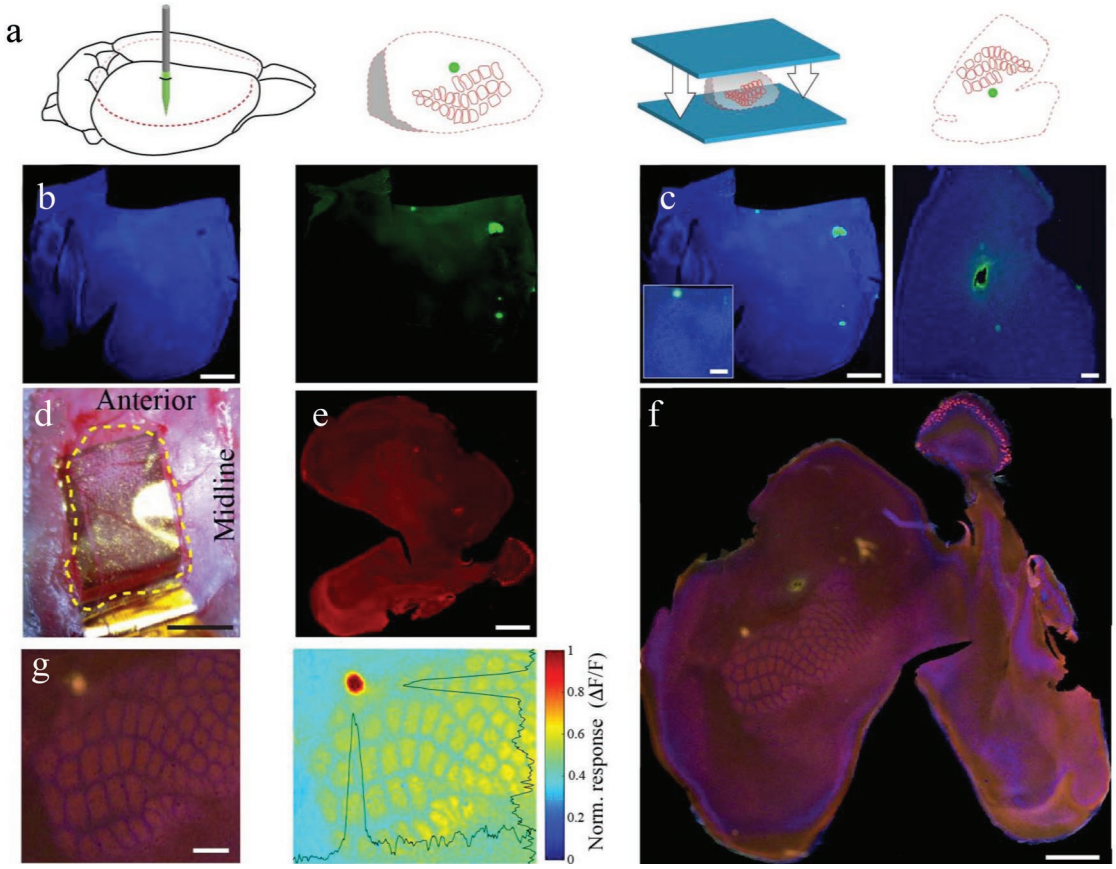

Figure 4. Multiwavelength fluorescence combining CS, DAPI, and vGLUT2 imaging to localize neural probes in vivo. a) Schematic for CS-based brain marking, cortical flattening, and slicing procedures. b) Fluorescence microscopy of flattened rat cortical slice to visualize DAPI staining (left) and CS marking (right). Scale bar 1 mm. c) Multiwavelength fluorescence microscopy images of CS marking implantation point on the surface of a flattened cortical slice (left) and deep cortex of a coronal slice (right). Scale bar 1 mm left, 300 µm inset, 300 µm right. d) Intra-operative micrograph demonstrating NeuroGrid array placed on the cortical surface of a postnatal day 14 mouse pup. Scale bar 2 mm. e) vGLUT2 immunohistochemistry reveals characteristic patterns in rodent barrel cortex. Scale bar 1 mm. f) Multiwavelength fluorescence microscopy images of CS marking edge of NeuroGrid placement on the cortical surface (yellow/green) relative to barrel cortex in a flattened cortical slice. Scale bar 1 mm. g) Magnified version of a portion of the image in (f) allowing allocation of NeuroGrid electrodes to different cortical regions (left) with normalized fluorescence response (right). Scale bar 200 µm.

Supporting Information). In addition, we coated 50 µm tungsten wires with CS (**Figure 5**a), implanted them into adjacent brain areas, and performed intra-operative neurophysiological recordings. The data obtained by coated and noncoated wires had similar quality and frequency content (Figure 5b,c), suggesting that CS does not interfere with the ability to record high-quality neurophysiological data from conventional neural interface devices.

Overall, we developed a comprehensive process to localize probes within neural tissue using the intrinsic fluorescence of CS. We characterized CS films and determined the additives and solution processing approaches to optimize stability and fluorescence. CS can be coated onto penetrating probes and introduced into neural tissue in a spatially restricted manner, localizing probes as small as 50 µm in deep brain tissue. It is also compatible with tissue processing techniques required for commonly used immunohistochemical and histological experimentation. Combining CS-based neural probe marking with a variety of routinely used fluorescence staining protocols allowed for efficient localization of high spatiotemporal resolution surface electrocorticography arrays. CS is biocompatible, inexpensive, and simple to prepare, providing a viable alternative to other methods of neural probe localization. Because CS is currently being incorporated into the structure of neural interface devices, approaches that maximize the utility of its intrinsic properties, such as fluorescence, have the potential to simplify and streamline the experimental procedures required to efficiently acquire, localize, and interpret neurophysiological signals.

Experimental Section

CS Preparation: CS (50–190 kD, 75–85% deacetylated) was purchased from Sigma-Aldrich. CS powder was added in 2% v/v acetic acid and left for 3 h at 70 °C to be dissolved. The resulting solution was filtered consecutively with 40 and 10 µm cell strainers. The filtered solution was concentrated via thermal dehydration (180 °C) to 2.5% w/v. The concentrated CS solution was used to create CS/GOPS solution with 2% v/v concentration and CS/PVA solution with 100% w/w concentration. Films of CS around 30 gauge metallic needles and 50 µm thick polyimide-coated tungsten microwires were created by dip-coating technique. The immersion speed determined the thickness of the film. Thicker CS films were achieved by multiple consecutive immersion-film drying cycles. CS/GOPS and CS/PVA solutions were drop cast on a petri dish and dried

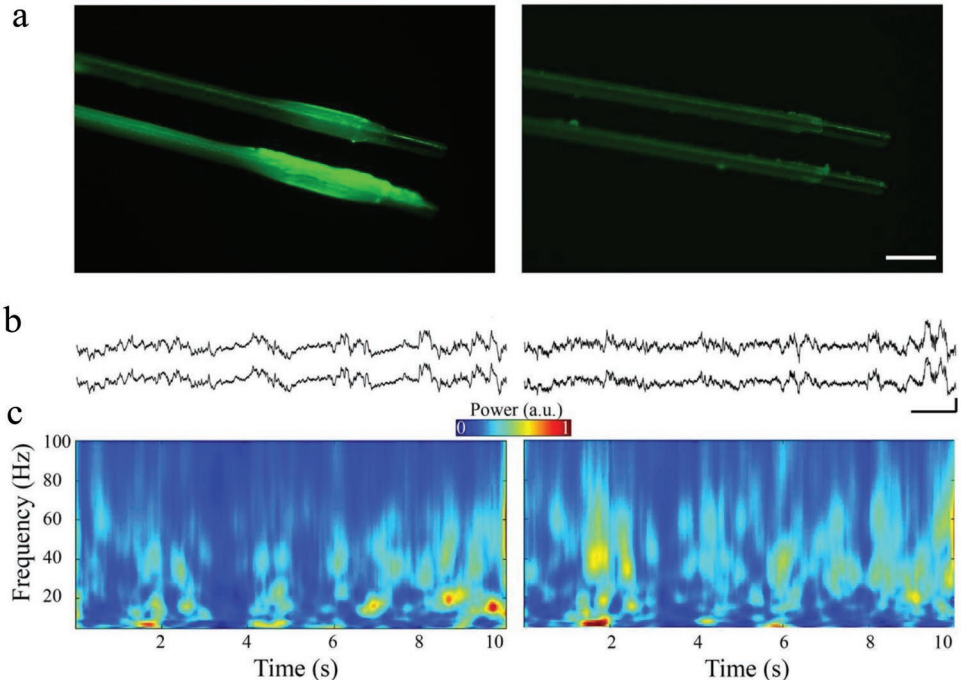

Figure 5. CS does not preclude acute neurophysiological recording in vivo. a) Fluorescence microscopy images showing CS-coated (left) and non-CS-coated (right) 50 µm tungsten wires for implantation and recording. Scale bar 200 µm. b) Sample raw traces acquired using CS-coated (left) and non-CS-coated (right) 50 µm tungsten wires during intra-operative anesthesia from adjacent brain regions. Scale bar 1 s, 500 µV. c) Sample spectrograms acquired using CS-coated (left) and non-CS-coated (right) 50 µm tungsten wires during intra-operative anesthesia demonstrating similar frequency content in adjacent brain regions.

at 60 °C to create a film. This thermal treatment fully cross-linked the GOPS, and eliminated the possibility of further reaction.[23,27,36]

In Vitro Procedures: Glass (SiO2) slides were first cleaned by applying acetone, isopropyl alcohol, and DI water. 0.5 mL of CS solution was then transferred onto a cleaned slide and spin coated at 1000 rpm for 30 s to create a thin film. The CS coating was incised in a straight line with a surgical scalpel to observe contrast between CS and the glass. Agarose gel was prepared using a heated and stirred solution of 3% v/w agarose powder (Sigma Aldrich) in PBS (Sigma Aldrich). 75 mm Petri dishes were filled with the agarose solution to a height of 5 mm and then refrigerated until the solution was gelatinized. Gelatinized agar was punctured multiple times in a square formation with ≈1 mm between punctures using either a parylene-coated 30 gauge metallic needle or a 50 µm thick tungsten wire dip-coated in a CS solution. The agar was then sliced at a thickness of 100 µm with a vibratome and imaged.

In Vivo Procedures: All animal experimentation was approved by the Institutional Animal Care and Use Committee at Columbia University Irving Medical Center. Male and female Long-Evans rats (8–15 weeks) and Swiss Webster mice (5–21 days) were used. Rodents were anesthetized with isoflurane and placed in a stereotactic frame for intracranial implantation. Craniotomies were drilled over one hemisphere, exposing the dorsal cortical surface of the brain from coronal suture anteriorly to lambdoid suture posteriorly. NeuroGrids consisting of 120 PEDOT:PSS-based electrodes embedded in a 4 µm thick parylene-C substrate were placed on the pial surface of the brain for neurophysiological recording.[23] At the conclusion of recording, rodents were euthanized with 100 mg kg^{-1} of sodium pentobarbital. CS-coated needles were stereotactically inserted perpendicular to the brain surface at the corners of the NeuroGrid arrays, and promptly removed. Rodents were perfused with 4% PFA and brains were extracted.

Tissue Processing: Brains were stored for 24–48 h in 4% PFA at 4 °C prior to transfer to PBS solution. Cortices were flattened after removal of the underlying midline structures as per previously described techniques[37,41] at room temperature (RT) and kept in 4% PFA for 24 h. The slices were then incubated for 1 h at RT in a blocking solution composed of PBS (0.01 M), 3% Normal Donkey Serum, and 0.3% Triton X-100. The slices were then transferred to a solution containing anti-Vesicular Glutamate Transporter 2 (VGlut2) polyclonal guinea-pig antibody (AB2251-I Sigma Millipore) in a 1:2000 dilution and kept overnight at 4 °C. Subsequently, the tissue was washed and incubated with secondary antibody, Alexa Fluor 594 AffiniPure Donkey Anti-guinea pig IgG (H+L) (706-585-148) from Jackson Immunoresearch at 1:1000 dilution. Lastly, the tissue was incubated with DAPI (D9542-5MG) from Sigma Aldrich at 0.2 µg mL^{-1} and after washing, the brain slices were mounted with Flouromount-G (00-4958-02, ThermoFisher).

Fluorescence Microscopy: Fluorescent images were captured and tiled using a computer-assisted camera connected to an ECHO Revolve microscope. The images were adjusted for brightness and contrast and assembled into panels using ImageJ and Adobe Illustrator.

Supporting Information

Supporting Information is available from the Wiley Online Library or from the author.

Acknowledgements

This work was supported by Columbia University Irving Medical Center Department of Neurology and Institute for Genomic Medicine, as well as Columbia University School of Engineering and Applied Science. G.D.S. was supported through the Human Frontiers Postdoctoral Fellowship Program. S.D. was supported by a Marie Sklodowska Curie Individual Fellowship (MSCA-IF-GF 799501). Additional funding was provided by a CURE Taking Flight Award. The authors thank all Khodagholy and Gelinas laboratory members for their support.

Conflict of Interest

The authors declare no conflict of interest.

Keywords

chitosan, fluorescence microscopy, neural interface devices, organic bioelectronics

Received: August 3, 2019
Revised: September 30, 2019
Published online:

[1] J. Rivnay, R. M. Owens, G. G. Malliaras, *Chem. Mater.* **2014**, *26*, 679.
[2] G. Lanzani, *Nat. Mater.* **2014**, *13*, 775.
[3] M. Berggren, A. Richter-Dahlfors, *Adv. Mater.* **2007**, *19*, 3201.
[4] J. W. Jeong, G. Shin, S. II Park, K. J. Yu, L. Xu, J. A. Rogers, *Neuron* **2015**, *86*, 175.
[5] H. Kim, C. H. Tator, M. S. Shoichet, *J. Biomed. Mater. Res., Part A* **2011**, *97A*, 395.
[6] M. N. V. Ravi Kumar, *React. Funct. Polym.* **2000**, *46*, 1.
[7] G. D. Spyropoulos, J. N. Gelinas, D. Khodagholy, *Sci. Adv.* **2019**, *5*, eaau7378.
[8] G. Kravanja, M. Primožič, Ž. Knez, M. Leitgeb, *Molecules* **2019**, *24*, 1960.
[9] B. Weng, J. Diao, Q. Xu, Y. Liu, C. Li, A. Ding, J. Chen, *Adv. Mater. Interfaces* **2015**, *2*, 1500059.
[10] H. M. Lee, M. H. Kim, Y. II Yoon, W. H. Park, *Mar. Drugs* **2017**, *15*, 105.
[11] H. Huang, F. Liu, S. Chen, Q. Zhao, B. Liao, Y. Long, Y. Zeng, X. Xia, *Biosens. Bioelectron.* **2013**, *42*, 539.
[12] W. Tang, T. Yan, J. Ping, J. Wu, Y. Ying, *Adv. Mater. Technol.* **2017**, *2*, 1700021.
[13] C. Diacci, J. W. Lee, P. Janson, G. Dufil, G. Méhes, M. Berggren, D. T. Simon, E. Stavrinidou, *Adv. Mater. Technol.* **2019**, *1*, 1900262.
[14] H. Wang, X. Ma, Y. Hao, *Adv. Mater. Interfaces* **2017**, *4*, 1.
[15] T. C. Tseng, L. Tao, F. Y. Hsieh, Y. Wei, I. M. Chiu, S. H. Hsu, *Adv. Mater.* **2015**, *27*, 3518.
[16] W. C. Huang, H. S. Chi, Y. C. Lee, Y. C. Lo, T. C. Liu, M. Y. Chiang, H. Y. Chen, S. J. Li, Y. Y. Chen, S. Y. Chen, *ACS Appl. Mater. Interfaces* **2019**, *11*, 11270.
[17] Z. X. Lim, K. Y. Cheong, *Adv. Mater. Technol.* **2018**, *3*, 1800007.
[18] R. Chen, A. Canales, P. Anikeeva, *Nat. Rev. Mater.* **2017**, *2*, 16093.
[19] G. Buzsáki, E. Stark, A. Berényi, D. Khodagholy, D. R. Kipke, E. Yoon, K. D. Wise, *Neuron* **2015**, *86*, 92.
[20] E. Krook-Magnuson, J. N. Gelinas, I. Soltesz, G. Buzsáki, *JAMA Neurol.* **2015**, *72*, 823.
[21] V. G. J. M. Vanderhorst, B. Ulfhake, *J. Chem. Neuroanat.* **2006**, *31*, 2.
[22] J. Lübke, D. Feldmeyer, *Brain Struct. Funct.* **2007**, *212*, 3.
[23] D. Khodagholy, J. N. Gelinas, T. Thesen, W. Doyle, O. Devinsky, G. G. Malliaras, G. Buzsaki, *Nat. Neurosci.* **2015**, *18*, 310.
[24] J. N. Gelinas, D. Khodagholy, T. Thesen, O. Devinsky, G. Buzsáki, *Nat. Med.* **2016**, *22*, 641.
[25] D. Khodagholy, T. Doublet, M. Gurfinkel, P. Quilichini, E. Ismailova, P. Leleux, T. Herve, S. Sanaur, C. Bernard, G. G. Malliaras, *Adv. Mater.* **2011**, *23*, H268.
[26] K. Tybrandt, D. Khodagholy, B. Dielacher, F. Stauffer, A. F. Renz, G. Buzsáki, J. Vörös, *Adv. Mater.* **2018**, *30*, 1706520.
[27] D. Khodagholy, J. N. Gelinas, G. Buzsáki, *Science* **2017**, *358*, 369.
[28] R. Fiáth, A. L. Márton, F. Mátyás, D. Pinke, G. Márton, K. Tóth, I. Ulbert, *Sci. Rep.* **2019**, *9*, 111.
[29] J. J. Jun, N. A. Steinmetz, J. H. Siegle, D. J. Denman, M. Bauza, B. Barbarits, A. K. Lee, C. A. Anastassiou, A. Andrei, Ç. Aydın, M. Barbic, T. J. Blanche, V. Bonin, J. Couto, B. Dutta, S. L. Gratiy, D. A. Gutnisky, M. Häusser, B. Karsh, P. Ledochowitsch, C. M. Lopez, C. Mitelut, S. Musa, M. Okun, M. Pachitariu, J. Putzeys, P. D. Rich, C. Rossant, W. Sun, K. Svoboda, M. Carandini, K. D. Harris, C. Koch, J. O'Keefe, T. D. Harris, *Nature* **2017**, *551*, 232.
[30] E. C. Jensen, *Anat. Rec.* **2012**, *295*, 2031.
[31] J. J. Dicarlo, J. W. Lane, S. S. Hsiao, K. Johnson, *J. Neurosci. Methods* **1996**, *64*, 75.
[32] L. Einarson, *Am. J. Pathol.* **1932**, *8*, 295.
[33] J. W. Salatino, K. A. Ludwig, T. D. Y. Kozai, E. K. Purcell, E. Lansing, M. Clinic, E. Lansing, E. Lansing, *Nat. Biomed. Eng.* **2017**, *1*, 862.
[34] R. M. Gold, G. Sumprer, H. M. Ueberacher, G. Kapatos, *Physiol. Behav.* **1975**, *14*, 861.
[35] R. P. Yezierski, R. M. Bowker, *J. Neurosci. Methods* **1981**, *4*, 53.
[36] D. Khodagholy, J. N. Gelinas, Z. Zhao, M. Yeh, M. Long, J. D. Greenlee, W. Doyle, O. Devinsky, G. Buzsáki, *Sci. Adv.* **2016**, *2*, e1601027.
[37] R. N. Strominger, T. A. Woolsey, *J. Neurosci. Methods* **1987**, *22*, 113.
[38] M. Liguz-Lecznar, J. Skangiel-Kramska, *Int. J. Dev. Neurosci.* **2007**, *25*, 107.
[39] N. Ichinohe, F. Fujiyama, T. Kaneko, K. S. Rockland, *J. Neurosci.* **2003**, *23*, 1372.
[40] C. C. H. Petersen, *Neuron* **2007**, *56*, 339.
[41] S. M. Lauer, U. Schneeweiß, M. Brecht, S. Ray, *J. Visualized Exp.* **2018**, e56992.